Journal for ImmunoTherapy of Cancer

Intraperitoneal administration of a modified vaccinia virus Ankara confers single-chain interleukin-12 expression to the omentum and achieves immune-mediated efficacy against peritoneal carcinomatosis

Ángela Bella,[1,2] Leire Arrizabalaga,[1,2] Claudia Augusta Di Trani,[1,2] Jose Gonzalez-Gomariz,[1,2] Celia Gomar,[1,2] Joan Salvador Russo-Cabrera,[1,2] Irene Olivera,[1,2] Assunta Cirella,[1,2] Myriam Fernandez-Sendin,[1,2] Maite Alvarez ,[1,2] Alvaro Teijeira ,[1,2] Cigdem Atay,[3] José Medina-Echeverz,[3] Maria Hinterberger ,[3] Hubertus Hochrein,[3] Ignacio Melero ,[1,2,4,5,6] Pedro Berraondo ,[2,4] Fernando Aranda [1,2]

To cite: Bella Á, Arrizabalaga L, Di Trani CA, *et al*. Intraperitoneal administration of a modified vaccinia virus Ankara confers single-chain interleukin-12 expression to the omentum and achieves immune-mediated efficacy against peritoneal carcinomatosis. *Journal for ImmunoTherapy of Cancer* 2023;**11**:e006702. doi:10.1136/jitc-2023-006702

► Additional supplemental material is published online only. To view, please visit the journal online (http://dx.doi.org/10.1136/jitc-2023-006702).

IM, PB and FA are joint senior authors.

Accepted 12 October 2023

For numbered affiliations see end of article.

Correspondence to
Dr Fernando Aranda;
faranda@unav.es

ABSTRACT

Background Peritoneal carcinomatosis is an advanced stage of cancer in which the disease has spread to the peritoneal cavity. In order to restore antitumor immunity subverted by tumor cells in this location, we evaluated intraperitoneal administrations of modified vaccinia virus Ankara (MVA) engineered to express single-chain interleukin 12 (scIL-12) to increase antitumor immune responses.

Methods MVA encoding scIL-12 (MVA.scIL-12) was evaluated against peritoneal carcinomatosis models based on intraperitoneal engraftment of tumor cells. CD8-mediated immune responses, elucidated antitumor efficacy, and safety were evaluated following intravenous, intratumoral, or intraperitoneal administration of the viral vector. The immune response was measured by ELISpot (enzyme-linked immunosorbent spot), RNA sequencing, flow cytometry, intravital microscopy, and depletion of lymphocyte subsets with monoclonal antibodies. Safety was assessed by body-weight follow-up and blood testing. Tissue tropism on intravenous or intraperitoneal administration was assessed by bioluminescence analysis using a reporter MVA encoding luciferase.

Results Intraperitoneal or locoregional administration, but not other routes of administration, resulted in a potent immune response characterized by increased levels of tumor-specific $CD8^+$ T lymphocytes with the ability to produce both interferon-γ and tumor necrosis factor-α. The antitumor immune response was detectable not only in the peritoneal cavity but also systemically. As a result of intraperitoneal treatment, a single administration of MVA.scIL-12 encoding scIL-12 completely eradicated MC38 tumors implanted in the peritoneal cavity and also protected cured mice from subsequent subcutaneous rechallenges. Bioluminescence imaging using an MVA encoding luciferase revealed that intraperitoneal administration targets transgene to the omentum. The omentum is considered a key tissue in immune protection of the peritoneal cavity. The safety profile of intraperitoneal administration was also better than that following intravenous administration since no weight loss or hematological toxicity was observed when the vector was locally delivered into the peritoneal cavity.

Conclusion Intraperitoneal administration of MVA vectors encoding scIL-12 targets the omentum, which is the tissue where peritoneal carcinomatosis usually begins. MVA.scIL-12 induces a potent tumor-specific immune response that often leads to the eradication of experimental tumors disseminated to the peritoneal cavity.

WHAT IS ALREADY KNOWN ON THIS TOPIC

⇒ Peritoneal carcinomatosis is an advanced stage of certain tumors with a dismal prognosis. The success of hyperthermic intraperitoneal chemotherapy highlights the relevance of locoregional therapeutic interventions.

WHAT THIS STUDY ADDS

⇒ We show that intraperitoneal administration of modified vaccinia virus Ankara encoding single-chain interleukin 12 confers expression of single-chain interleukin 12 to the omentum, enhancing the antitumor effect while limiting the toxicity in models of peritoneal carcinomatosis.

HOW THIS STUDY MIGHT AFFECT RESEARCH, PRACTICE OR POLICY

⇒ Our findings highlight the importance of omentum in triggering an immune response against peritoneal carcinomatosis.

BACKGROUND

Peritoneal carcinomatosis (PCa) is an advanced stage of tumor spread in the peritoneal cavity, frequently occurring in end-stage ovarian and colon cancer.[1–5] Tumor cells exfoliated from primary tumors or metastases disseminate through the peritoneal cavity. Among the different tissues found in the peritoneum, the omentum reportedly plays a critical role in the balance between tumor dissemination and the endogenous immune response against the tumor.[6–8] First, certain characteristics of the omentum such as the high level of vascularization, fat storage, and potential for tissue regeneration promote nesting of tumor cells. Second, the omentum contains immune aggregates called 'milky spots' responsible for immune defense against pathogens (mainly viruses and bacteria) invading the peritoneum.[9 10] These omental immune cells may be subverted by tumor cells to comprise an immunosuppressive microenvironment.[11–13] Palliative treatment of PCa is based on chemotherapy, cytoreductive surgery, or hyperthermic intraperitoneal chemotherapy.[14–16] Despite these advances, PCa remains a condition with an extremely poor prognosis. Experimental therapies are being evaluated for PCa, in several immunotherapy clinical trials using immunostimulatory monoclonal antibodies, adoptive transfer of T lymphocytes, cytokines, or Toll-like receptor agonists.[4 17–19] Unfortunately, clinical results have been unsatisfactory, and advances from preclinical research efforts are needed.

Viruses represent interesting tools in cancer immunotherapy since several of their molecular components are easily detected by pattern recognition receptors leading to the activation of an antiviral immune response that can be redirected to the tumor.[20] In particular, modified vaccinia virus Ankara (MVA) is an attenuated cytopathic strain whose dsDNA is recognized by both the Toll-like receptor 9 and the Stimulator of Interferon Genes pathway.[21 22] Genetic engineering allows antigens to be expressed in the context of the danger signals elicited by MVA, a vector which studies have shown to be an excellent vaccine platform.[23–25] The Food and Drug Administration has recently approved an MVA-based smallpox vaccine. Tumor-associated antigens have also been introduced into MVA to create therapeutic antitumor vaccines.[26] Tumor antigen transgenes have been evaluated either alone or co-expressed with other immunostimulatory molecules such as CD40L or CD137L.[24 26] Here, we study the antitumor effect in PCa models of MVA encoding a single-chain interleukin 12 (scIL-12) construct alone. IL-12 is a potent immunostimulatory cytokine that leads to the activation of natural killer cells (NK), Th_1 CD4 T lymphocytes, CD8 T lymphocytes, and macrophages.[27–30] Early reports of unacceptable toxicity associated with the intravenous administration of recombinant IL-12 have led to the development of different clinical strategies to localize the activity of IL-12 to the tumor microenvironment.[31–33] Due to its efficacy/safety balance, IL-12 is often part of local and intratumoral strategies.[34 35]

In this study, we report how MVA readily targets the omentum, and how its transgene expression is observed mainly in this critical tissue where IL-12 mounts an effector immune response against PCa. In this strategy, there is no need to identify tumor antigens since an endogenous in situ vaccine effect is sought.[21] Expression of scIL-12 by MVA following intraperitoneal administration generates a potent adaptive cytotoxic T lymphocyte-mediated immune response against tumor spread in the peritoneal cavity, achieving an effective antitumor effect.

METHODS

Cell lines and culture media

The MC38 colon cancer cell line was obtained from Dr Karl E. Hellström (University of Washington, Seattle) and was grown in Roswell Park Memorial Institute 1640 medium (RPMI) with GlutaMAX supplemented with 10% fetal bovine serum (FBS), 100 U/mL penicillin, 100 µg/mL streptomycin and 50 µM β-mercaptoethanol (Gibco, Thermo Fisher Scientific, Waltham, Massachusetts, USA). The ID8.*Vegf*/GFP ovarian cancer was obtained from Dr George Coukos (Ludwig cancer research, Switzerland) and was grown in Dulbecco's modified Eagle's, high-glucose medium (Invitrogen, Carlsbad, California, USA) supplemented with 4% FBS (Gibco, Thermo Fisher Scientific), 100 U/mL penicillin, 100 µg/mL streptomycin (Gibco, Thermo Fisher Scientific), 5 µg/mL insulin, 5 µg/mL transferrin, and 5 ng/mL sodium selenite (Roche, Indianapolis, Indiana, USA). The CT26 colon cancer cell line was purchased from American Type Culture Collection (CRL-2638 cell lines). CT26 cells were cultured in RPMI GlutaMax medium supplemented with 10% FBS, 100 U/mL penicillin, 100 µg/mL streptomycin, and 50 µM β-mercaptoethanol (Gibco, Thermo Fisher Scientific). All cell lines were grown in a humidified incubator with 5% CO_2 at 37°C for at least 7 days before injection into mice and were tested regularly for mycoplasma contamination.

MVA-BN recombinant vectors

MVA-BN was developed by Bavarian Nordic and is deposited in the European Collection of Cell Cultures (V00083008). All recombinant MVA molecules were generated from a cloned version of MVA-BN on a bacterial artificial chromosome. The infectious viruses were reconstituted from artificial bacterial chromosomes by transfection of bacterial artificial chromosome DNA into BHK-21 cells and superinfecting them with the Shope fibroma virus as a helper virus. After three additional passages of primary embryo fibroblasts, helper virus-free MVA recombinant viruses were obtained. All viruses used in animal experiments were purified twice through a sucrose cushion.

In vitro characterization of MVA.scIL-12

Splenocytes were infected with increasing amounts of MVA.empty or MVA encoding scIL-12 (MVA.scIL-12)

(50% tissue culture infectious dose ($TCID_{50}$): 0.3; 1.25; 2.5 or 5). After 24 hours, supernatants were collected and analyzed for IL-12 concentration. Tumor cells (MC38, CT26, and ID8.*Vegf*/GFP) were seeded and infected with MVA.empty or MVA.scIL-12 ($TCID_{50}$: 5), 48 hours later, supernatants were collected, and IL-12 was quantified. Splenocytes were incubated with tumor-cell-derived-supernatant containing 1,000, 100, or 10 ng/mL of IL-12 for 48 hours, and interferon (IFN)-γ production was assessed in supernatants.

Flow cytometry analysis

A single-cell suspension of tissue/organs collected at the indicated times was stained. Splenocytes and peritoneal cell single-cell suspensions were first stained with the R-PE-labeled Pro5 H-2Kb Pentamer $MuLV_{622\text{-}629}$ (KSPWFTTL) (ProImmune Ltd, Oxford, UK) in the presence of FcR-Block (anti-CD16/32 clone 93 BioLegend, San Diego, California, USA) following the manufacturer's instructions. Then, single-cell suspensions were stained with Zombi NIR Fixable viability kit (BioLegend) as a LIVE/DEAD marker prior to staining of surface or intracellular markers using the following fluorochrome-labeled antibodies (BioLegend): anti-CD3-AF647 (17A2), anti-CD8-BV510 (53–6.7), anti-CD19-BV650 (6D5), anti-CD45.2-PerCPCy5.5 (104), anti-CD107a-FITC (1D4B), anti-IFN-γ-PE (XMG1.2) and anti-TNF-α-BV421 (MP6-XT22). For IL-12 detection, splenocytes or a single-cell suspension derived from tumor-bearing omentum were stained with with Zombi NIR, anti-CD3-AF647 (17A2), anti-CD8-BV510 (53–6.7), anti-CD19-BV650 (6D5), anti-CD45-PECy7 (30-F11), anti-CD4-FITC (GK1.5), anti-CD11b-PerCPCy5.5 (M1/70), anti-CD11c-BV605 (N418), anti-F4/80-BV421 (BM8) and anti-NK1.1-PE-Dazzel594 (Pk136) followed by intracellular staining with anti-IL-12(p40)-PE (C15.6) or an isotype control antibody. Fluorescence minus one or biological comparison controls were used for cell analysis. Flow cytometry analysis was performed using a CytoFLEX S or CytoFLEX LX apparatus (Beckman Coulter, Miami, Florida, USA). Data analysis was performed using FlowJo software (TreeStar, Ashland, Oregon, USA).

Animal experimentation

In vivo experiments were carried out with 6–8 weeks old female C57BL/6 mice purchased from Harlan Laboratories (Barcelona, Spain). The mice were kept under specific pathogen-free conditions. The experimental design was approved by the Ethics Committee for Animal Testing of the University of Navarra (033–20, 038–20, 063–21, and 014–21). Exponentially growing MC38, CT26, and ID8.*Vegf*/GFP cells were trypsinized and prepared as a single-cell suspension in ice-cold phosphate-buffered saline (PBS). The animals were injected intraperitoneally with 300 µL of tumor cell suspension MC38 (5×10^5 cells), CT26 (2×10^5 cells), and ID8.*Vegf*/GFP (1×10^6 cells). In the case of the subcutaneous tumor model, mice were injected subcutaneously with 5×10^5 MC38 cells. Seven days after tumor cell inoculation (5 days in case of ID8.*Vegf*/GFP), mice were randomized and treated intraperitoneally, intravenously, or subcutaneously with 5×10^7 $TCID_{50}$ of the respective recombinant or PBS (control group). For the combinatorial therapy with anti-programmed death-ligand 1 (PD-L1), mice were treated with 200 µg of the antibody anti-PD-L1 (B7-H1; clone 10F.9G2; Bio X Cell) by intraperitoneal administrations on days +1, +3 and +6 post treatment. InVivoMAb polyclonal rat IgG was used as a control. Mice inoculated with tumor cells intraperitoneally were weighed and closely monitored for the development of ascites three times a week. Mice were sacrificed if body weight reached 28 g or clear signs of pain and distress appeared. For mice with subcutaneous tumor implants, tumor volume was measured three times a week. They were sacrificed according to the experimental design approved by the Ethics Committee for Animal Testing of the University of Navarra.

Omentectomy

For the surgical removal of the omentum, 5 weeks-old mice were first anesthetized and then secured in the supine posture. Under sterile conditions, a 1.5 cm incision was made in the abdomen to expose the greater curvature of the stomach and omentum. Both lateral ends of the omentum were cauterized for subsequent removal. Following this procedure, the abdominal wall was closed using surgical sutures and surgical glue. In the *Sham* control, the same steps as described above were followed. The omentum was carefully lifted and then placed back in the abdominal cavity.

Lymphocyte population depletions

The tumor model and treatment regimen were as in the antitumor activity assay, but mice were depleted of $CD8^+$ T cells using anti-CD8β (Ly 3.2; clone H35-17.2, Bio X Cell), $CD4^+$ T using anti-CD4 (clone GK1.5, Bio X Cell), and NK cells using anti-mouse NK1.1 (clone PK136, Bio X Cell). InVivoMAb rat IgG2a (clone 2A3, Bio X Cell) or InVivoMAb polyclonal rat IgG was used as a control. 200 µg of each antibody were administered per mouse intraperitoneally (*i.p.*) on two consecutive days before the first treatment and on days 2, 6, 9, and 13 (2, 6, 9, 13, 16, 20, and 24 for NK1.1) after treatment to maintain immune cell depletion during the experiment.

Samples processing

Peritoneal washings, spleen, and omentum were collected after 3 mL of pre-chilled PBS injection (2% FBS) into the peritoneal cavity. After a gentle massage of the peritoneum to remove any attached cells, a 23G needle was used to collect all the fluid. The peritoneal washings were frozen at −80°C for further analysis. The spleens were mechanically disaggregated and filtered through a 70 µm cell strainer (Thermo Fisher Scientific, Waltham, Massachusetts, USA). Splenocytes and peritoneal cells were depleted of erythrocytes, and single-cell suspensions were kept at 4°C until further analysis by

enzyme-linked immunosorbent spot (ELISpot) or flow cytometry. Omenta were weighed and frozen in RNAlater Stabilization Solution at −80°C until RNA isolation for RNA sequencing (RNA-seq). For flow cytometry analysis of omentum, tumor-bearing omenta were also cut into small sections and digested with 3–5 mL of 0.075% collagenase IV for 10 min at 37°C. The reaction was stopped by adding 50 µl of EDTA, and cells were forced through a cell strainer, centrifuged and washed with PBS+2% FBS. Erythrocyte depletion was performed if needed.

Cytokine analyses

IFN-γ and IL-12 in serum and the peritoneal washings of mice were assayed by ELISA (BD OptEIA catalog #555138 and #555256, San Diego, California, USA), following the manufacturer's instructions. Data were analyzed and interpolated into standard curve values using GraphPad Prism.

ELISpot analysis was performed using mouse an IFN-γ ELISpot assay kit (BD-Biosciences catalog #551083, San Diego, California, USA). Ninety-six-well plates were coated with 100 µl of assay diluent containing anti-IFN-γ monoclonal Ab and incubated overnight at 4°C. The plates were washed and then blocked with RPMI-1640 medium containing 10% FBS for 3 hours at room temperature. Splenocytes depleted of erythrocytes were added to the wells (5×10^5) and stimulated with the $p15E_{604\text{-}611}$ peptide (10 µg/mL), $AH1_{6\text{-}14}$ peptide (10 µg/mL), 5×10^4 irradiated tumor cells of MC38 or CT26 (20,000 rads) in 200 µl/well. Before use, MC38 or CT26 tumor cells as a stimulator were treated with 500 IU/mL of IFN-γ for 24 hours to increase major histocompatibility complex (MHC)-I expression. After 24 hours of incubation with stimulators, IFN-producing cells were measured by ELISpot according to the manufacturer's instructions.

MVA biodistribution

Mice were *i.p.* injected with 5×10^7 $TCID_{50}$ recombinant MVA-expressing luciferase. Six, 24, 48, and 72 hours after injection, mice were anesthetized and 100 µl of luciferin (Promega, Madison, Wisconsin, USA) (20 mg/mL) was administered *i.p.* After 5 min, in vivo bioluminescence was detected using a PhotonIMAGER TM (Biospace Lab, Paris, France). At time point 6 hours post injection, 5 min after luciferin administration mice were euthanized and the spleen, omentum, and mesentery of each mouse were collected for ex vivo bioluminescence detection. Data were analyzed using M3 Vision software. For the study of the in vivo biodistribution of MVA.scIL-12, MC38 tumor-bearing mice received intraperitoneal treatment at day 7 and 3 hours after treatment, mice were injected *i.p.* with 0.5 mg of Brefeldin A (Merck KGaA, Darmstadt, Germany) diluted in PBS. At time point 6 hours post treatment, mice were euthanized and tumor-bearing omenta were processed for flow cytometry analysis.

RNA-seq

Total RNA extraction from the omentum was performed using the RNeasy Mini Kit (Qiagen, Hilden, Germany), following the manufacturer's recommendations. The concentration and RNA integrity of the samples were determined using the Qubit RNA HS (High Sensitivity) Assay Kit (Invitrogen, Waltham, Massachusetts, USA) and the Agilent 2200 TapeStation (Agilent Technologies, Santa Clara, California, USA). Library preparation was performed using the Illumina Stranded mRNA Prep Ligation kit following the manufacturer's protocol. All sequencing libraries were constructed from 100 ng of total RNA according to the manufacturer's instructions. Briefly, the protocol selects and purifies poly(A) containing RNA molecules using magnetic beads coated with poly(T) oligos. Poly(A)-RNAs are fragmented, and reverse transcribed into the first cDNA strand using random primers. The second cDNA strand is synthesized in the presence of deoxyuridine triphosphate to ensure strand specificity. Resulting cDNA fragments are purified with AMPure XP beads (Beckman Coulter), adenylated at 3′ ends and then ligated with uniquely indexed sequencing adapters. Ligated fragments are purified and PCR amplified to obtain the final libraries. Libraries were then sequenced using a NextSeq2000 sequencer (Illumina, San Diego, California, USA). 40–50 million pair-end reads (100 bp; Rd1:51; Rd2:51) were sequenced for each sample and demultiplexed using Cutadapt. RNA-seq was carried out at the Genomics Unit of the Center for Applied Medical Research (CIMA, Universidad de Navarra). Quality control of all samples was performed with the FastQC tool (http://www.bioinformatics.bbsrc.ac.uk/projects/fastqc). Before alignment, low-quality reads and adapters were removed using Trimmomatic V.0.39.[21] The mouse reads were mapped to the mm36 assembly using the STAR aligner V.2.7.9a[22] with the mm39 assembly and annotated with Gencode V.M27. Raw counts were quantified with featureCounts V.2.0.[36] In order to identify viral reads in the RNA-seq data, unmapped reads were mapped to the MVA viral genome (ASM645792v1) using Bowtie2 V.2.4.2,[37] and a read count was performed using featureCounts V.2.0. The differentially expressed gene analysis was carried out in R/Bioconductor following the bioinformatics workflow provided by edgeR.[38] First, genes with fewer than five counts in all samples (non-expressed genes) were removed from the analysis before normalization. The data sets were normalized using the normalization of the TMM (trimmed mean of M values), then the log2CPM values were calculated, and the normalized expression matrix was used for statistical analysis. We selected the set of genes differentially expressed for each comparison using the criteria of adjusted p value<0.05% and false discovery rate <0.05%. Gene set enrichment analysis (GSEA) was performed with fgsea[39] using the gene sets M5-GO: BP and C7-IMMNUNESIGDB from MSigDB V.7.4 database.[24] Before running GSEA, the lists of expressed genes were preranked by their log2FC value without any type of filtering. GSEA against C7-IMMUNESIGDB was

performed after converting mouse genes to their human homologs. The fgsea output was filtered keeping those enriched pathways with an adjusted p value<0.05% and re-ranked by their gene Ratio. Data are available on the Gene Expression Omnibus website (accession number: GSE226991).

Intravital microscopy

For intravital microscopy of omenta in ID8.*Vegf*/GFP tumors engrafted in the peritoneal cavity of hCD2-RFP mice, 1×10^6 cells were injected *i.p.* in 300 µl of PBS. Two weeks later, mice were treated with MVA.empty or MVA.scIL-12. For intravital confocal microscopy, the omentum was surgically exposed. The temperature of the mice was monitored by a rectal probe connected to a heating blanket (Kemp) and mice were kept asleep under Isoflurane anesthesia (2%). Mice were placed on a custom-built stage and imaged with an LSM880 inverted microscope (Zeiss) equipped with a 25X water immersion objective (NA, 0.8). Imaging sessions took from 2 to 4 hours per mice and time-lapse acquisitions lasted from 30 min to 2 hours with frames taken every 2 min. Several tumor foci (GFP^+) were imaged per session and mice. Images and time-lapse videos were analyzed using the IMARIS (Bitplane) software.

Histological analysis

Omenta were removed, immediately formalin fixed and paraffin embedded. Two consecutive sections (3 µm thick) were stained with H&E and CD8 (rabbit monoclonal, clone D4W2Z, Cell Signaling, 98941). Immunohistochemical staining was performed using the EnVision+System (K400311-2, Agilent) according to the manufacturer's recommendations. Antigen retrieval was first performed for 30 min at 95°C in 0.01 M Tris-1 mM EDTA buffer (pH=9). For $CD8^+$ area quantification, FIJI software and a "brown detection area" macro were used.

Statistical analysis

GraphPad Prism V.8.2.1 software (GraphPad Software, San Diego, California, USA) was used for statistical analysis. Data were analyzed by one-way analysis of variance followed by Sidak's multiple comparison test. Longitudinal data were fitted to a third-order polynomial equation and compared with an extra sum of squares F test with Bonferroni adjustment for multiple comparisons. Survival analysis was performed using the logarithmic rank test. P values<0.05 were considered statistically significant.

RESULTS

Locoregional administration of MVA.scIL-12 generates a tumor-specific immune response leading to 100% tumor eradication in a model of colon cancer PCa

We generated a new non-replicative MVA vector encoding an scIL-12 without any tumor-associated antigen. Incubation of MVA.scIL-12 to infect mouse splenocytes induced the release of scIL-12 into the supernatants in a dose-dependent manner (online supplemental figure 1A,B). We studied the expression of MVA.IL-12 in the various immune populations of infected splenocytes using flow cytometry, revealing a high percentage of $IL\text{-}12^+$ cells, primarily in dendritic cells and macrophages (online supplemental figure 1C). In addition, MVA.scIL-12 infected MC38, CT26, and ID8.*Vegf* tumor cell lines and resulted in the release of scIL-12 into the supernatants (online supplemental figure 1A,D). Moreover, when culture supernatants from infected MC38 cells were added to mouse splenocytes, they produced IFN-γ. This demonstrates that MVA.scIL-12 expresses bioactive IL-12 (online supplemental figure 1E). In vivo, intraperitoneal administration of MVA.scIL-12 but not MVA.empty led not only to local IL-12 production detected in the peritoneal wash, but also to detectable presence in sera, suggesting a systemic biodistribution of the immunomodulatory cytokine (online supplemental figure 1F). Maximum levels of IL-12 were detected in sera 6 hours after administration of the viral vector, and these rapidly declined thereafter, becoming undetectable after 48 hours. Consistently, serum IFN-γ induced by transgenic IL-12 in vivo peaked 48 hours after vector administration, therefore confirming the bioactivity of the secreted cytokine in vivo (online supplemental figure 1G).

To evaluate the antitumor activity mediated by MVA.scIL-12, we used a PCa model induced by the administration of colon cancer MC38 cells in the peritoneal cavity. Twenty-four hours after *i.p.* treatment, the viral vectors themselves (MVA.empty and MVA.scIL-12) lead to an increase in the myeloid cell compartment in peritoneal lavages. However, the vector expressing IL-12 counters this expansion and demonstrates a lower percentage of the myeloid compartment. Reducing myeloid suppressor cells and macrophages within the peritoneal cavity may prove advantageous in promoting an effective $CD8^+$ T cell-mediated antitumor response (online supplemental figure 2). Interestingly, administration of MVA encoding scIL-12 induced a high number of $IFN\text{-}\gamma^+$ T lymphocytes reactive to the MHC class I endogenous retroviral $p15E_{604\text{-}611}$ antigen expressed by the tumor cells and to cultured MC38 cells (figure 1A). Despite the presence of the tumor, empty MVA did not induce tumor-specific T-cell responses (figure 1B). Furthermore, $CD8^+$ T lymphocytes from the spleen and the peritoneal wash were analyzed by flow cytometry. MVA.scIL-12 significantly increased the frequency of antigen-specific $CD8^+$ T cells (figure 1C) as detected locally and systemically in the mice. Moreover, treatment resulted in a significant increase of the percentage of lytic $CD107a^+CD8^+$ cells able to produce both IFN-γ and tumor necrosis factor α (TNF-α) (figure 1D). This potent adaptive immune response correlated with a strong therapeutic antitumor response that could be observed on day 14 by the absence of hemorrhagic ascites and on day 23 by the lack of macroscopical tumor nodules in the peritoneum of mice treated with MVA.scIL-12 (figure 1E). Long-term

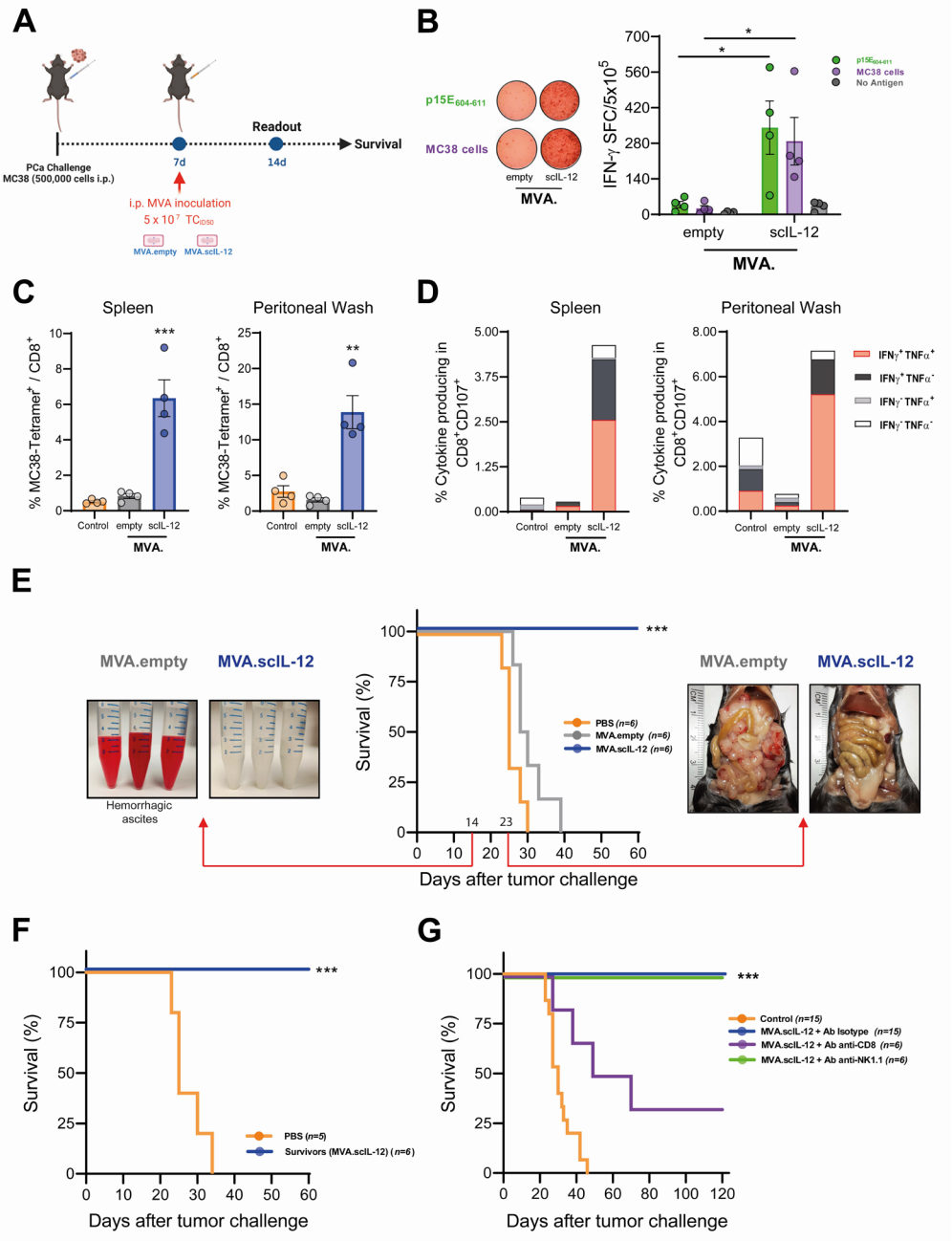

Figure 1 Intraperitoneal administration of MVA.scIL-12 induces a potent antitumor-specific immune response in the MC38 colon cancer model of peritoneal carcinomatosis. (A) C57BL/6 mice were challenged *i.p.* with 5×10^5 MC38 colon cancer cells. Seven days later, mice were treated *i.p.* with PBS (control) or 5×10^7 $TCID_{50}$ of the indicated MVA constructs. Mice were followed to assess survival or some mice were sacrificed 1 week after vector inoculation, and splenocytes and peritoneal washing fluids were collected to assess antitumor immune response. (B) IFN-γ–producing cells measured by ELISpot in splenocytes stimulated with the $p15E_{604-611}$ antigen, or with colon cancer cells. (C) Percentage of gp70 tetramer$^+$ in the $CD8^+$ T lymphocytes in the spleen and the peritoneal washing fluids. (D) Percentage of cells producing IFN-γ, TNF-α in $CD8^+$ T lymphocytes in the spleen and the peritoneal washing fluids. (E) Kaplan-Meier survival curve and representative images of the peritoneal washing fluids on day 14 or of the peritoneum on day 23. (F) Mice that eliminated tumor cells were rechallenged with an intraperitoneal injection of 5×10^5 MC38 cells. The Kaplan-Meier survival curve is shown. (G) C57BL/6 mice were challenged *i.p.* with 5×10^5 MC38 colon cancer cells. Seven days later, mice were treated *i.p.* with PBS (control) or 5×10^7 $TCID_{50}$ of MVA.scIL-12. The treated mice received an irrelevant antibody or an antibody to deplete $CD8^+$ T, $CD4^+$ T lymphocytes or NK cells on days –2, 0, 2, 6, 9, and 13 (additional doses on days 16, 20, and 24 for NK cells depletion), being 0 the day of the start of treatment. Kaplan-Meier survival curve is shown. Data are expressed as mean±SEM. The results are representative of two independent experiments. Two-way ANOVA was performed followed by Sidak's post-test. **p<0.01; ***p<0.005. ANOVA, analysis of variance; ELISpot, enzyme-linked immunosorbent spot; IFN, interferon; *i.p.*, intraperitoneal; MVA, modified vaccinia virus Ankara; MVA.scIL-12, MVA encoding scIL-12; NK, natural killer; PBS, phosphate-buffered saline; PCa, peritoneal carcinomatosis; scIL-12, single-chain interleukin 12; $TCID_{50}$, 50% tissue culture infectious dose; TNF, tumor necrosis factor.

follow-up of mice revealed that 100% of the mice which received scIL-12-engineered MVA survived (figure 1E). To evaluate whether locoregional treatment elicited T-cell memory, mice that had eradicated peritoneal implants were rechallenged intraperitoneally with MC38 cells. All mice that had previously rejected MC38 on MVA.scIL-12 intraperitoneal treatment were resistant to rechallenge and survived until the end of the experiment. In contrast, all the untreated control animals succumbed due to intraperitoneal tumor progression by day 40 (figure 1F).

To interrogate the immune cells involved in the antitumor effect, depleting monoclonal antibodies against $CD8^+$ T lymphocytes, $CD4^+$ T lymphocytes or NK/NKT cells were used concomitantly with MVA.scIL-12 (figure 1G). The antitumor effect was significantly reduced by $CD8^+$ depletion, although not completely abolished. The depletion of $CD4^+$ T or NK cells alone had no impact on overall survival. Therefore, CD8 T cells are strictly required for the antitumor effect but probably act together with other mechanisms to achieve maximum efficacy.

Locoregional administration of MVA.scIL-12 provides a better antitumor effect than intravenous administration

Locoregional administration entails several drawbacks, and its use must be justified and clearly be beneficial for the patient. Therefore, we compared this route of administration with the more commonly used intravenous (*i.v.*) injection. Interestingly, *i.v.* administration of MVA.scIL-12 showed worse antitumor activity (figure 2A). Notably *i.v.* treated mice showed signs of toxicity associated with the systemic expression of scIL-12. These include significant weight loss that was detected 2 and 4 days after *i.v.* vector administration, unlike when *i.p.* injection was used (figure 2B). Furthermore, hematologic toxicity was also detected, as reflected by the reduced numbers of circulating platelets 24 hours and 72 hours following MVA vector administration (figure 2C). The *i.p.* and *i.v.* routes similarly decreased the number of circulating white blood cells (figure 2D). To explain the therapeutic superiority of the *i.p.* route, we studied locoregional and systemic concentrations of scIL-12 and IFN-γ. The *i.v.* route induced very high circulating levels of both cytokines, while *i.p.* administration gave rise to lower levels of both cytokines in sera (figure 2E). Focusing on the peritoneal cavity, *i.p.* administration induced a significantly higher increase in the concentrations of IL-12 and IFN-γ in peritoneal wash fluid as compared with *i.v.* administration (figure 2F).

The peritoneal and splenic percentages of $p15E_{604\text{-}611}$ specific $CD8^+$ T cells induced by MVA.scIL-12 in treated tumor-bearing mice were significantly increased if compared with MVA.empty. Of note, *i.v.* administration of MVA.scIL-12 did not increase the numbers of tumor-specific T-cells in the peritoneum and inconsistently increases were observed in the spleen (figure 2G). These results were confirmed using IFN-γ ELISpot assays testing responses to $p15E_{604\text{-}611}$ tumor-antigen and MC38 cells (figure 2H).

Combinatorial treatment or repeated *i.p.* administration of MVA.scIL-12 improves antitumor effectiveness in aggressive PCa models

To extend our observations to other models of PCa, CT26 colon cancer cells and ID8.*Vegf*/GFP ovarian cancer cells were used. While a single administration of MVA.scIL-12 exerted a significant antitumor effect against both PCa models, the antitumor effect was improved by the combination of anti-PD-L1 (figure 3A) or three repeated doses of the vector (figure 3B). In the CT26 model, the combination of MVA.scIL-12 plus PD-L1 blockade had a synergistic antitumor effect (figure 3A), and three doses of MVA.scIL-12 delayed tumor-induced death in all mice, and 38% completely eradicated the tumors (figure 3B). In the case of ID8 ovarian cancer, the combination of MVA.scIL-12 plus PD-L1 blockade was not superior to monotherapy (figure 3A), and repeated administration achieved 12.5% tumor-free mice at the end of the experiment (figure 3B). *I.p.* MVA.scIL-12 treatment increased tumor-specific T lymphocytes in CT26-bearing mice (online supplemental figure 3), as previously observed in the MC38 model. These results indicate that the beneficial effects of locoregional MVA.scIL-12 can be generated in aggressive PCa models.

Locoregional administration of MVA.scIL-12 attains more effective antitumor activity than intratumoral administration

We decided to compare the intratumoral (*i.t.*) and *i.p.* routes in terms of efficacy. For this purpose, MC38 cells were inoculated subcutaneously (*s.c.*), and 7 days later, the tumor was treated by single *i.t.* administration of MVA.scIL-12. Such a treatment had a significant effect on tumor growth, delaying the death of all mice and achieving a cure of approximately 30% of injected tumors (online supplemental figure 4A). Nevertheless, *i.t.* treatment was less efficacious than the *i.p.* route when the MC38 lesions grew disseminated in the peritoneum. The routes of administration were compared regarding the systemic effects (figure 4A).

Locoregional treatment of mice with *i.p.* or *s.c.* tumors achieved the maximum efficacy, with a high percentage of mice cured from their tumors (group C, blue). Intraperitoneal administration also exerted control when the MC38 tumor was only growing subcutaneously (group D, purple). Finally, *i.t.* treatment in the *s.c.* and *i.p.* tumor model was only able to control the *s.c.* tumors, but had only minimal effects on the peritoneal tumor (group B, gray). As previously shown, 100% of mice which eradicated the tumors in the peritoneum after *i.p.* treatment were able to reject the rechallenge of *s.c.* MC38 cells (online supplemental figure 4B). However, among those mice that eradicated the subcutaneous tumor after *i.t.* administration, only 65% were able to reject a rechallenge administered *i.p.* (online supplemental figure 4C). Therefore, we can conclude that the *i.p.* route results in a more powerful local and systemic immune memory response which is greater than that of other routes of administration. To demonstrate the relevance of the tumorous presence in

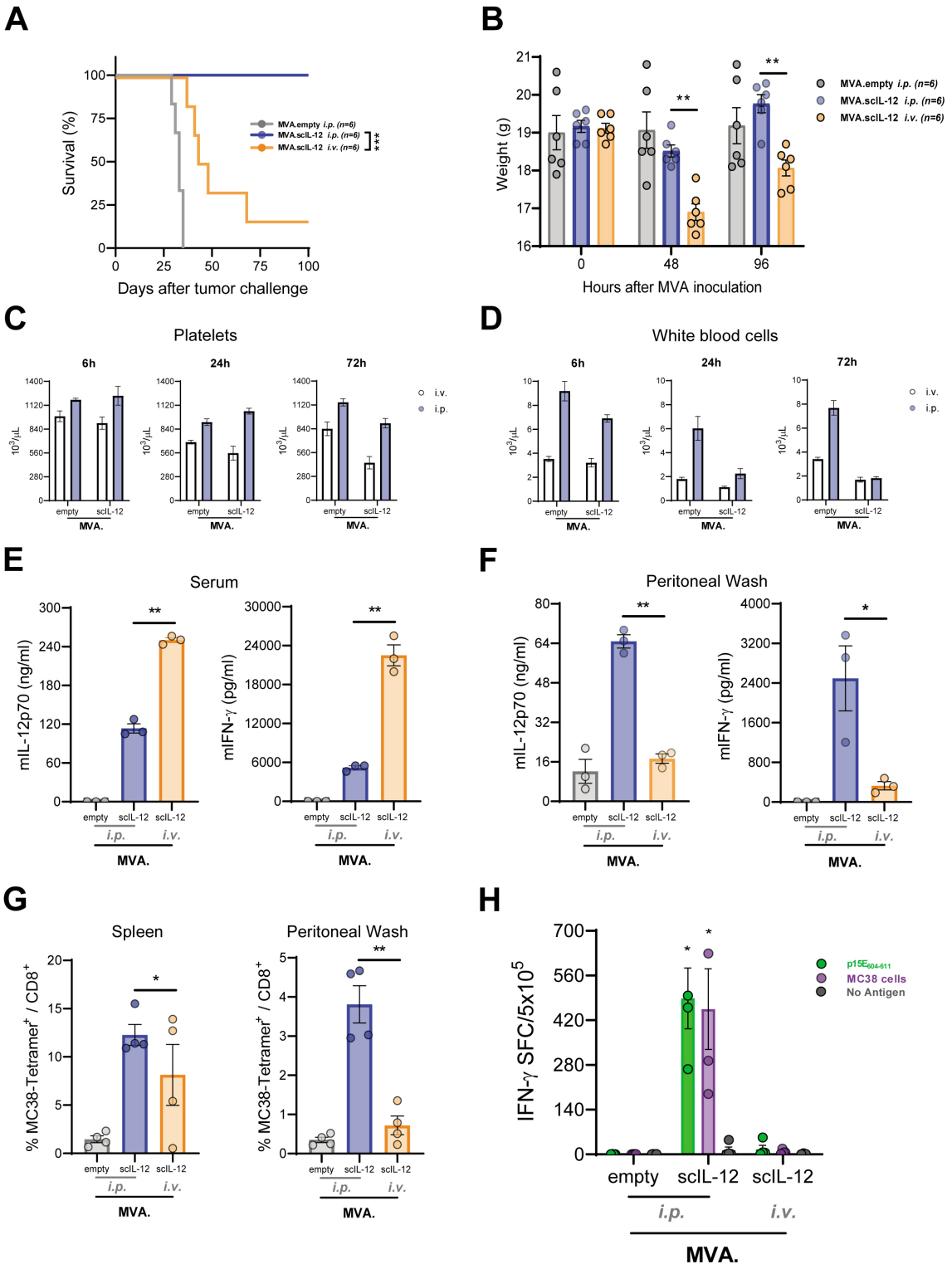

Figure 2 The intraperitoneal route of administration of MVA.scIL-12 is more efficacious than the intravenous route of administration. (A) C57BL/6 mice were challenged *i.p.* with 5×10^5 MC38 colon cancer cells. Seven days later, mice were treated *i.p.* with 5×10^7 $TCID_{50}$ of MVA.empty or MVA.scIL-12 or *i.v.* with 5×10^7 $TCID_{50}$ of MVA.scIL-12. The Kaplan-Meier survival curve is shown. (B) Body weight follow-up 48 hours and 96 hours after vector inoculation. (C) Platelets and (D) white blood cells 6 hours, 24 hours, or 72 hours after vector administration. (E) Concentration of IL-12 and IFN-γ 6 hour after vector inoculation in serum or in (F) peritoneal washing fluids. (G) Percentage of gp70 tetramer$^+$ in CD8$^+$ T lymphocytes in the spleen and the peritoneal washing fluids. (H) IFN-γ–producing cells measured by ELISpot in splenocytes stimulated with the antigen $p15E_{604-611}$ or with colon cancer cells. Data are represented as mean±SEM. Two-way ANOVA followed by Sidak's post-test. *p<0.05; **p<0.01; ANOVA, analysis of variance; ELISpot, enzyme-linked immunosorbent spot; IFN, interferon; *i.p.*, intraperitoneal; *i.v.*, intravenous; MVA, modified vaccinia virus Ankara; MVA.scIL-12, MVA encoding scIL-12; scIL-12, single-chain interleukin 12; $TCID_{50}$, 50% tissue culture infectious dose.

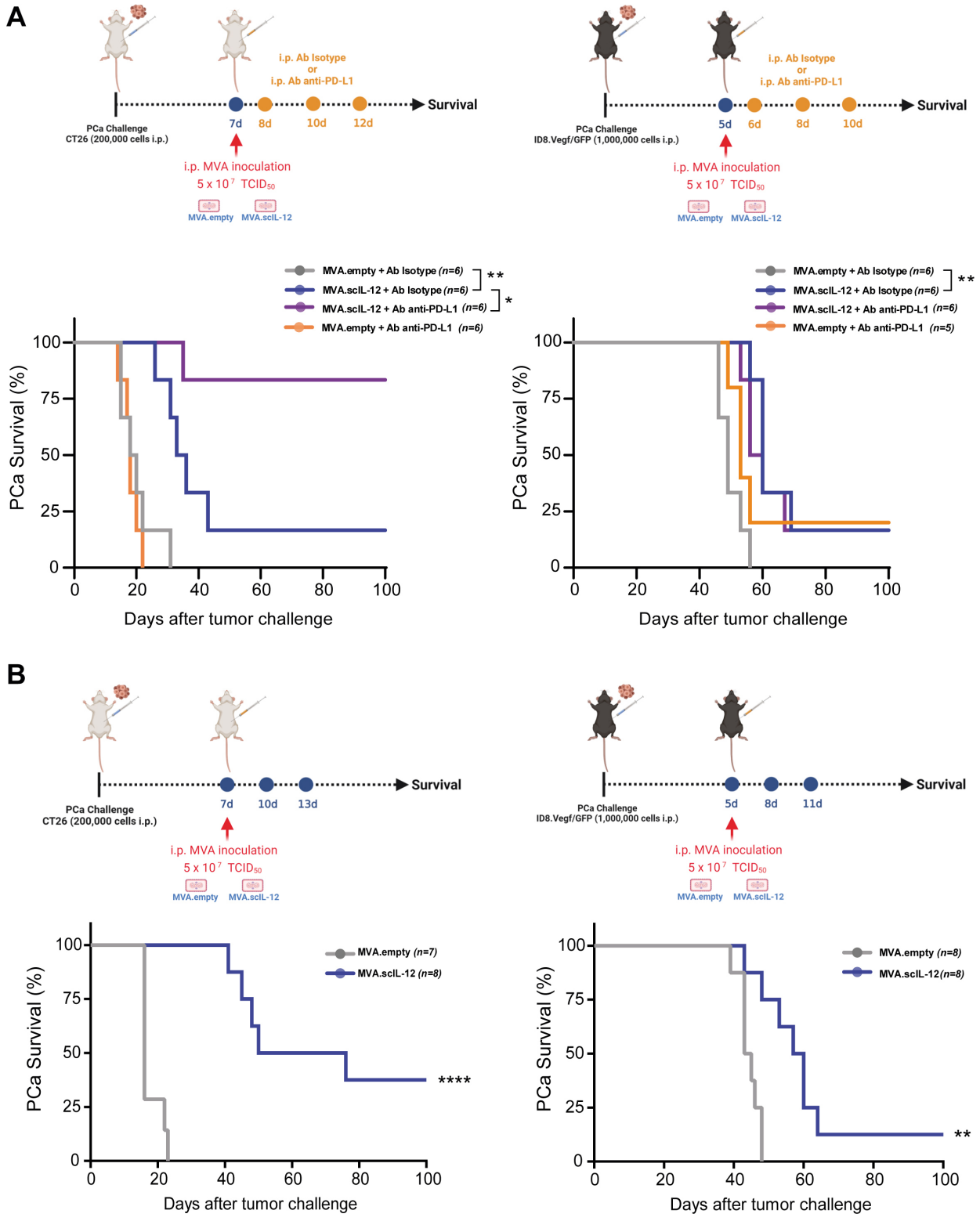

Figure 3 Combination with anti-PD-L1 and dose-dependence of the antitumor efficacy of MVA.scIL-12 against aggressive PCa mouse models. (A) BALB/c mice were challenged *i.p.* with 2×10^5 CT26 colon cancer cells. Seven days later, mice were treated *i.p.* with 5×10^7 $TCID_{50}$ of MVA.empty or MVA.scIL-12. C57BL/6 mice were challenged *i.p.* with 1×10^6 ID8.*Vegf*/GFP ovarian cancer cells. Five days later, mice were treated *i.p.* with 5×10^7 $TCID_{50}$ of MVA.empty or MVA.scIL-12. Mice were treated in combination with 200 µg of the antibody anti-PD-L1 by *i.p.* administrations on days +1, +3, and +6 post-MVA treatment. InVivoMAb polyclonal rat IgG (Isotype) was used as a control. The Kaplan-Meier survival curves are shown. (B) As in A, vectors were administered on days 7, 10, and 13 (CT26) or on days 5, 8, and 11 (ID8.*Vegf*/GFP). Data are represented as mean±SEM. Log-rank test. *p<0.05; **p<0.01; ****p<0.0001. *i.p.*, intraperitoneal; MVA, modified vaccinia virus Ankara; MVA.scIL-12, MVA encoding scIL-12; PCa, peritoneal carcinomatosis; PD-L1, programmed death-ligand 1; scIL-12, single-chain interleukin 12; $TCID_{50}$, 50% tissue culture infectious dose.

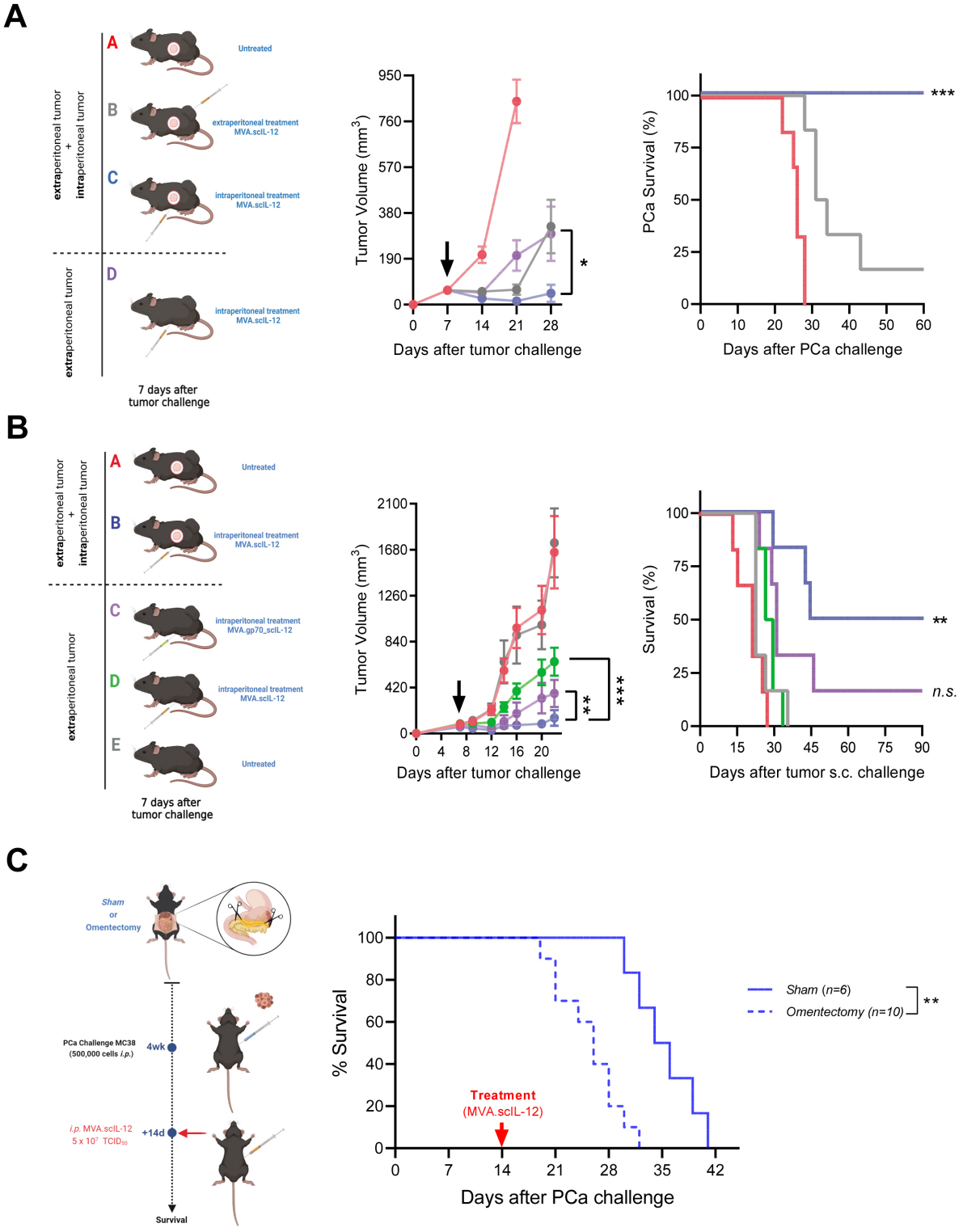

Figure 4 Treatment of intraperitoneal metastases with MVA.scIL-12 induces effective locoregional and distant antitumor therapeutic responses. (A) C57BL/6 mice were challenged *s.c.* and *i.p.* with 5×10^5 MC38 colon cancer cells or only *s.c.* Seven days later, the mice were left untreated or treated *i.t.* or *i.p.* with 5×10^7 $TCID_{50}$ of MVA.scIL-12. The mean tumor volume over time and the Kaplan-Meier survival curve are shown. (B) As in A, but including an additional experimental group that carried subcutaneous tumors and was treated on day 7 with 5×10^7 $TCID_{50}$ of MVA.gp70_scIL-12. (C) Four weeks after the surgical removal of the omentum, mice were challenged *i.p.* with 5×10^5 MC38 and treated with 5×10^5 $TCID_{50}$ of MVA.scIL-12 on day 14 after the PCa challenge. The Kaplan-Meier survival curves are shown. Data are represented as mean±SEM. Tumor volume data were fitted to a third-order polynomial and compared using extra sum-of-squares F test. Kaplan-Meier survival curves were analyzed using the log-rank test. *p<0.05, **p<0.01, ***p<0.001. *i.p.*, intraperitoneal; *i.t.*, intratumoral; MVA, modified vaccinia virus Ankara; MVA.scIL-12, MVA encoding scIL-12; PCa, peritoneal carcinomatosis; *s.c.*, subcutaneously; scIL-12, single-chain interleukin 12; $TCID_{50}$, 50% tissue culture infectious dose.

the peritoneum for the initiation of a systemic immune response, we constructed an MVA vector that encodes both scIL-12 and the tumor-associated antigen gp70. The antitumor effect against an *s.c.* tumor was evaluated after *i.p.* administration of the vectors. The vector encoding the tumor-associated antigen gp70 (MVA.gp70_scIL-12) exerted stronger antitumor effects as compared with the vector encoding only scIL-12 (figure 4B). To further investigate this locoregional antitumor activity, an omentectomy experiment was conducted. After the surgical intervention (4 weeks) mice were challenged *i.p.* with MC38 and treated with MVA.scIL-12 on day 14 after the PCa initiation. This time point was chosen to evaluate the efficacy of MVA.scIL-12 in a more aggressive model. The results demonstrated a significant delay in survival in the *Sham* group (with intact omentum) compared with the omentectomy group, highlighting the importance of the omentum in MVA-based immunotherapies (figure 4C).

Intraperitoneal MVA selectively distributes to the omentum and this phenomenon impacts on the immune response

To further understand the reason underlying the superior efficacy of the *i.p.* route of administration, we characterized the gene-transfered organs using an MVA encoding luciferase after *i.v.* or *i.p.* administration to tumor-free mice. Maximum luciferase expression was detected 6 hours after *i.p.* administration returning to baseline levels 72 hours later (figure 5A). After *i.v.* injection, the organ showing the most intense levels of bioluminescence was the spleen. The signal in the omentum and mesentery was 10 times less intense. In contrast, *i.p.* administration led to an intense signal in the omentum. The luminescence in the mesentery and spleen was detectable but 10 times lower in tumor-free (figure 5B) and tumor-bearing mice (online supplemental figure 5A). These results are highly relevant in PCa since the omentum is the first organ where *i.p.* delivered tumor cells home. In fact, macroscopic tumor nodules were observed in the excised omentum of mice sacrificed on day 15 after MC38 inoculation. MVA.scIL-12 *i.v.* treatment reduced the tumor size of tumor nodules, but the most efficacious treatment was MVA.scIL-12 *i.p.* In the latter case, no tumor nodules were visible, and enlarged milky spots indicated a powerful ongoing immune response locally in the omentum (online supplemental figure 5B).

The capacity of MVA to infect the omentum was also assessed by RNA-*seq*. Transcriptomic analysis of omenta from MC38-bearing mice in the peritoneum injected with MVA.empty or MVA.scIL-12 given *i.p.* revealed the presence of multiple viral mRNAs (figure 5C). Interestingly, no significant differences were observed in terms of viral transcripts between the two vectors, indicating that IL-12 expression does not affect virus infection (figure 5C). To further investigate MVA.scIL-12 targeting in the omentum, the IL-12 expression in tumor-bearing omentum was assessed by flow cytometry. IL-12 was detected in both hematolymphoid ($CD45^+$) cells and non-immune ($CD45^-$) cell populations which include tumor cells (figure 5D).

As can be seen in figure 6A, the expression of the proinflammatory cytokine IL-12 impacted multiple cellular processes and modulated the expression of genes involved in immune responses. MVA.scIL-12 administration induced a unique clearly distinct transcriptomic profile when compared with the MVA.empty administration (figure 6B). We also comparatively studied the differences between MVA.scIL-12 *i.p.* versus MVA.scIL-12 *i.v.* (figure 6C,D), and the differences with the untreated group (online supplemental figure 6A–D). This analysis identified the upregulation of several pathways involved in cellular metabolism and indicated a decrease of the presence of macrophages (figure 6E and online supplemental figure 7), and B cells (figure 6F and online supplemental figure 8).

Increased number and enhanced performance of lymphocytes in the omentum after MVA.scIL-12 treatment

We used multiphoton intravital confocal microscopy to assess the effects of intraperitoneal injection of MVA.scIL-12 in the omentum of ID8.*Vegf*/GFP tumor-bearing mice. In experiments set up as described in figure 7A, ID8.*Vegf*/GFP tumor cells homed to the omentum of hCD2RFP transgenic mice and were located mostly in the vicinity of fat-associated lymphoid clusters, and tumor cells were increased in numbers and size over time (figure 7A). Fifteen days post tumor cell inoculation, the malignant tissue showed poor T-cell infiltration, but there was interactions between T-cell and tumor-antigen (GFP^+) loaded macrophages ($F4/80^+$) located in the omentum (figure 7B, online supplemental video 1). Forty-eight hours after *i.p.* treatment with MVA.scIL-12, hCD2-RFP lymphocytes infiltrated more efficiently the tumor microenvironment than MVA.empty, resulting in a higher percentage of hCD2-RFP T cells contacting with tumor cells (figure 7C, online supplemental video 2). To validate this finding, we performed immunohistochemistry analysis of $CD8^+$ T lymphocytes in the omentum 24 hours and 7 days after treatment of tumors implanted in the peritoneal cavity 7 days before. In control mice that received saline, an overt infiltration was detected at day 8, but the T cell presence in the tumor microenvironment significantly decreased 22 days after tumor implantation, reflecting an active immunoediting process. Administration of MVA.empty did not modify the infiltration at any of the analyzed time points while MVA.scIL-12 markedly increased the infiltration of CD8 T cells as early as 24 hours after MVA administration. T-cell infiltration remained elevated for 7 days, and only a slight reduction in T lymphocytes was detected (figure 7D). Therefore, IL-12 expression by MVA in the omentum remodeled the immune landscape in this critical organ for the development of peritoneal carcinomatosis.

DISCUSSION

To explore novel therapeutic interventions that can contribute to improving the poor prognosis of PCa, we

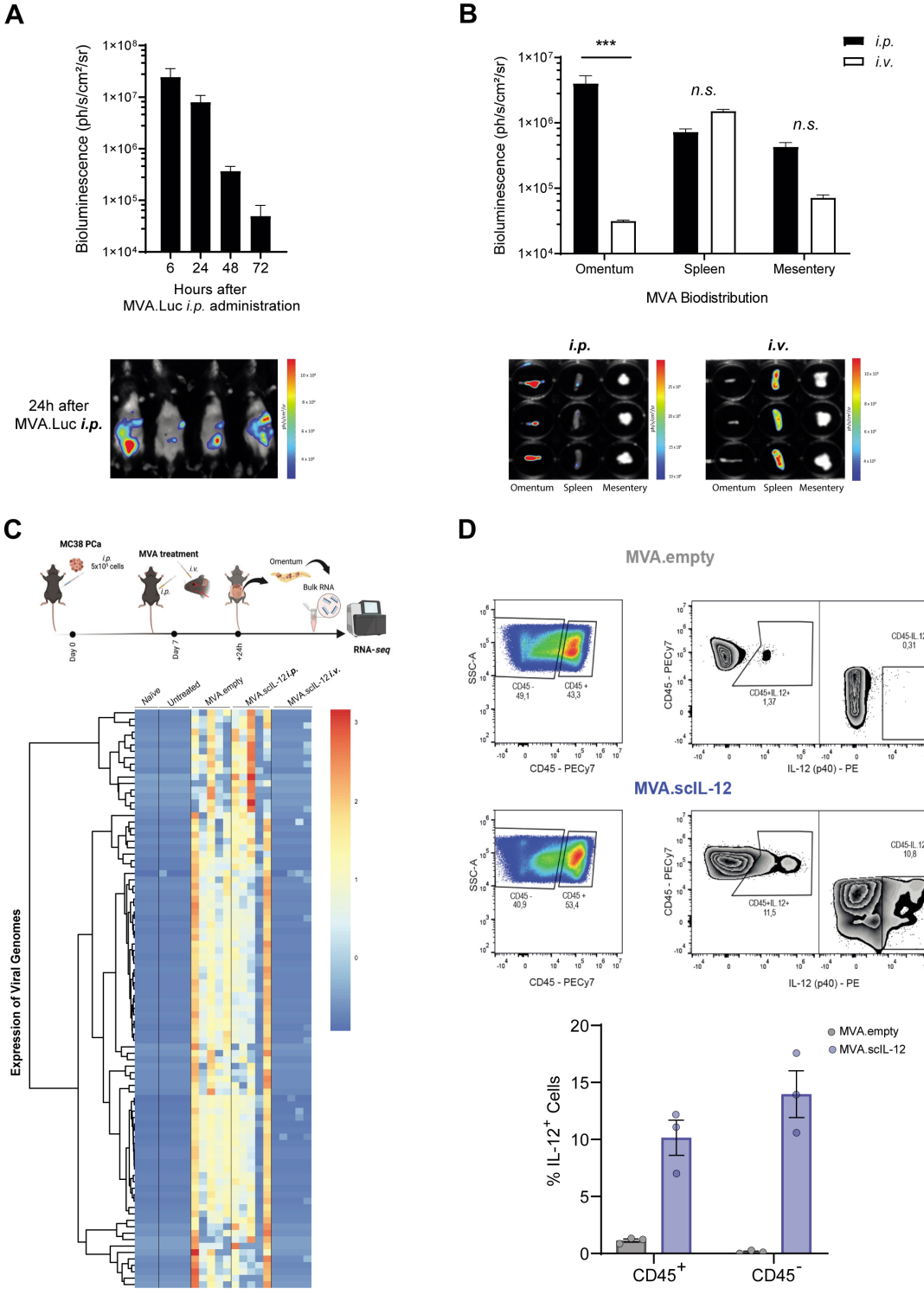

Figure 5 MVA infection and gene-transfer localize to the omentum following intraperitoneal administration. (A) C57BL/6 mice were injected *i.p.* with 5×10^7 $TCID_{50}$ of MVA.luciferase (MVA.Luc). Bioluminescence was monitored 6, 24, 48, and 72 hours after vector inoculation. A representative image at 24 hours is shown. (B) C57BL/6 mice were injected *i.p.* or *i.v.* with 5×10^7 $TCID_{50}$ of MVA.Luc. Six hours later, the omentum, spleen, and mesentery were isolated and bioluminescence was quantified. Data are represented as mean±SEM. Two-way ANOVA followed by Sidak's multiple comparisons test. (C) C57BL/6 mice were challenged *i.p.* with 5×10^5 MC38 colon cancer cells. The "naïve" group did not receive tumor cells or treatment. Seven days later, mice were treated *i.p.* with PBS, or 5×10^7 $TCID_{50}$ of MVA.empty or MVA.scIL-12. An additional group was treated *i.v.* with 5×10^7 $TCID_{50}$ of MVA.scIL-12. Twenty-four hours later, the omenta were isolated and analyzed by RNA-*seq*. Expression of viral genes in the omenta. (**D**) Representative plots and percentage of $CD45^+$ and $CD45^-$ cells expressing IL-12 in tumor-bearing omentum are shown. ANOVA, analysis of variance; *i.p.*, intraperitoneal; *i.v.*, intravenous; MVA, modified vaccinia virus Ankara; MVA.scIL-12, MVA encoding scIL-12; PBS, phosphate-buffered saline; RNA-*seq*, RNA sequencing; scIL-12, single-chain interleukin 12; $TCID_{50}$, 50% tissue culture infectious dose.

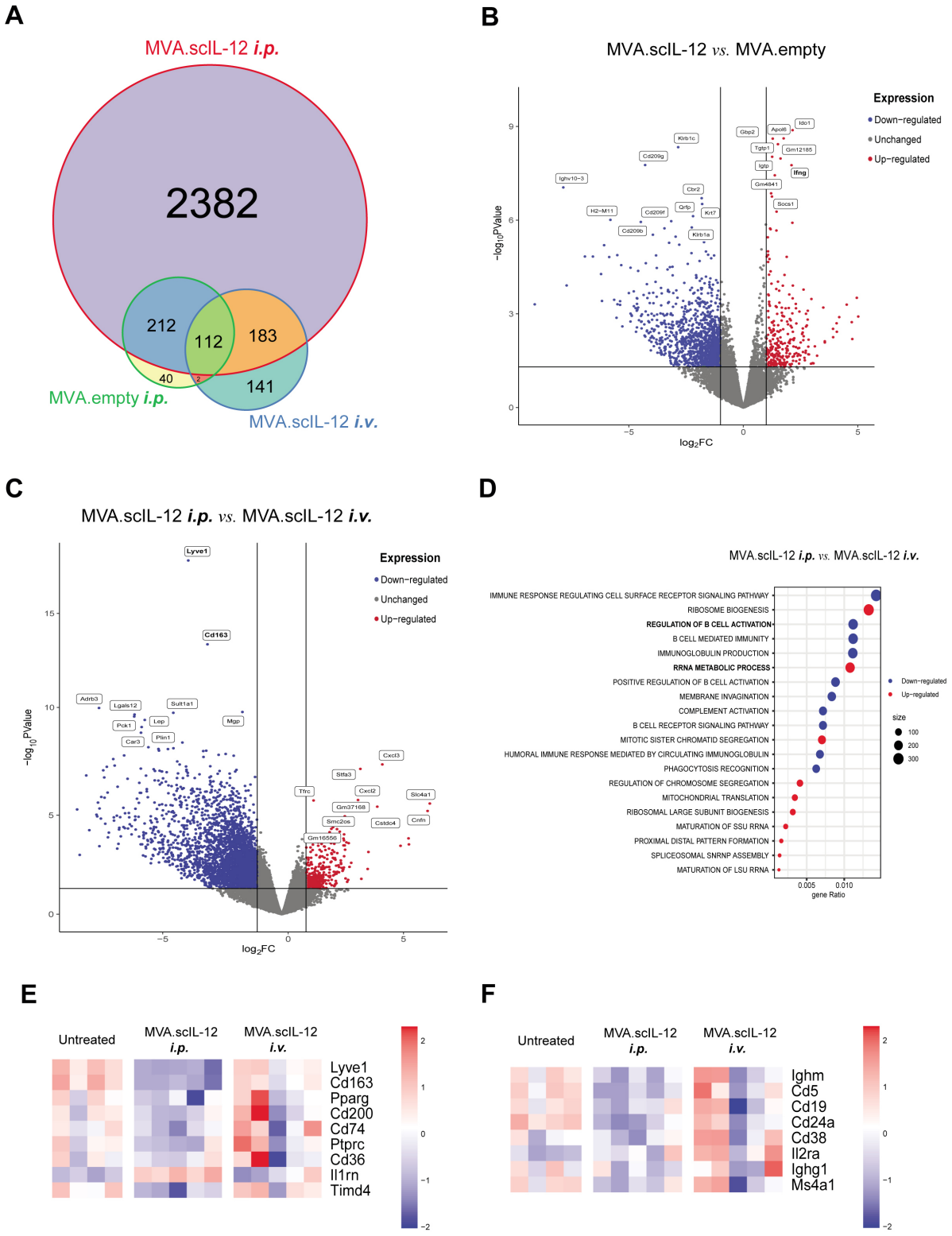

Figure 6 Modulation of the immune response in the omentum after locoregional administration of MVA.scIL-12 by RNA-*seq* analysis. (A) Venn diagram comparing differentially expressed genes (p value<0.05% and false discovery rate (FDR)<0.05%) in the different experimental groups described in figure 4C. (B) Volcano plots of differentially expressed genes of mice treated with MVA.scIL-12 *i.p.* versus MVA.empty-treated tumors. Red and blue dots indicate upregulated or downregulated genes, respectively, with a FDR<0.05. (C) Volcano plots of differentially expressed genes of MVA.scIL-12 *i.p.*-treated mice versus MVA.scIL-12 *i.v.*-treated tumors. Red and blue dots indicate upregulated or downregulated genes, respectively, with a FDR<0.05. (D) Gene Set Enrichment Analysis showing top 10 upregulated and downregulated GO:BP terms (p value adjusted<0.05%) (F) Heatmap of macrophage-related genes. (G) Heatmap of B-cell-related genes. *i.p.*, intraperitoneal; *i.v.*, intravenous; MVA, modified vaccinia virus Ankara; MVA.scIL-12, MVA encoding scIL-12; RNA-*seq*, RNA sequencing; scIL-12, single-chain interleukin 12.

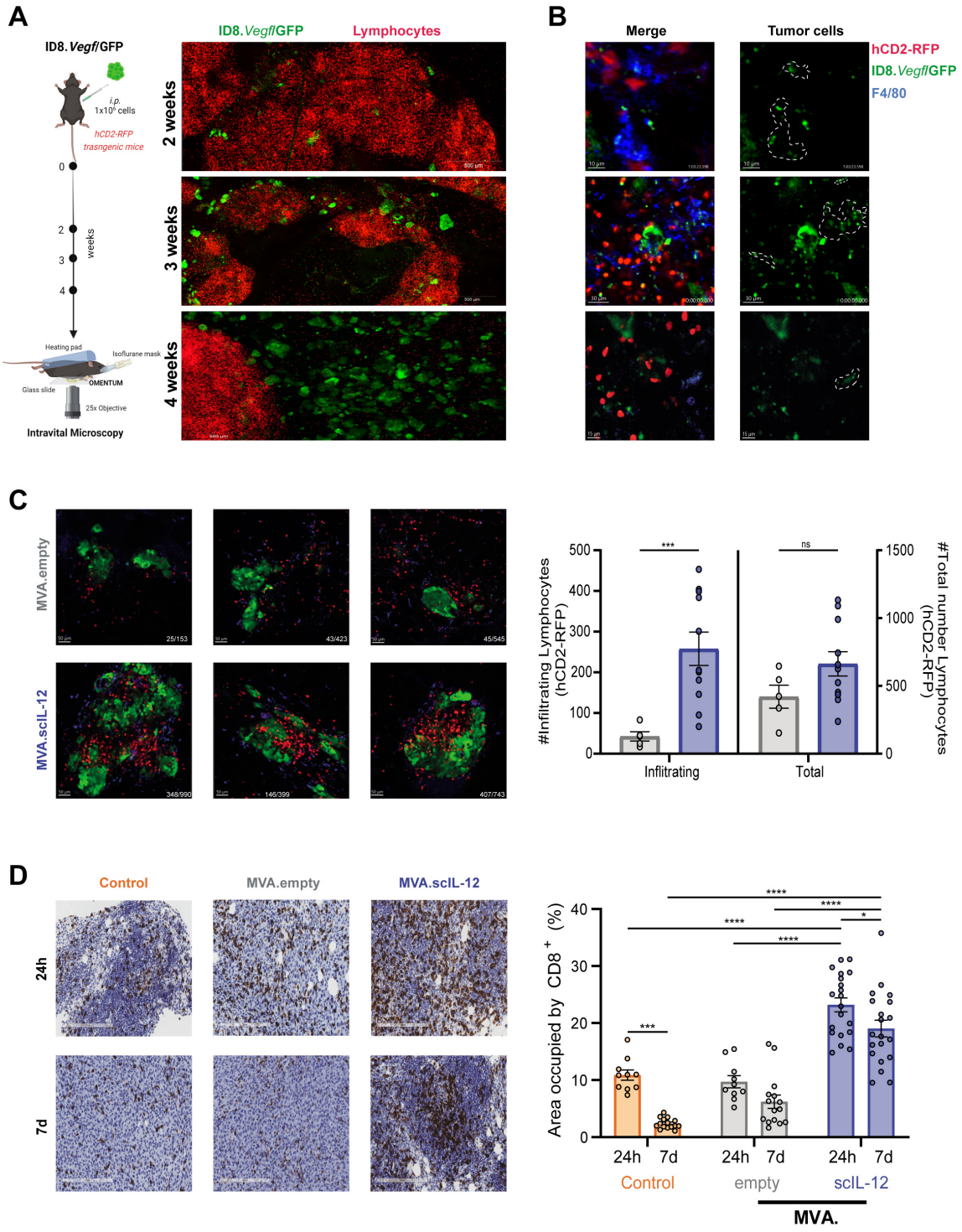

Figure 7 Intravital imaging and immunohistochemistry of tumor and immune cells in the omentum under treatment with intraperitoneal MVA.scIL-12. (A) Schematic representation of the model. Briefly, transgenic hCD2-RFP mice were challenged with 1×10^6 ID8.*Vegf*/GFP tumor cells and omentum was studied by intravital microscopy over time. Representative microphotographs of fluorescent green tumor cells and RFP^+ T cells within omenta at 2, 3 and 4 weeks after tumor implantation. (B) Representative microphotographs of macrophages F4/80$^+$ (Alexa Fluor 647, blue) bearing tumor material (GFP^+) 15 days after tumor inoculation (C) Representative microphotographs and quantification of T cells (RFP^+) infiltrating tumor lesion (GFP^+) 48 hours after MVA.empty or MVA.scIL-12 administration to 2 week tumor-bearing mice. Data are represented as mean±SEM. Mann-Whitney U tests. ***p<0.001. (D) Representative microphotographs and quantification of $CD8^+$ T cells infiltrating tumor lesion 24 hours and 7 days after PBS (control), MVA.empty or MVA.scIL-12 administration to 1 week MC38 tumor-bearing mice. Each dot represents a different zoomed area (20×) from three different mice. Data are represented as mean±SEM. Two-way ANOVA was performed followed by Sidak's post-test. *p<0.05; ***p<0.001; ****p<0.0001. ANOVA, analysis of variance; MVA, modified vaccinia virus Ankara; MVA.scIL-12, MVA encoding scIL-12; PBS, phosphate-buffered saline; scIL-12, single-chain interleukin 12.

have evaluated the antitumor efficacy of intraperitoneal administrations of MVA expressing scIL-12. An oncolytic vaccinia vector (GL-ONC1) has previously been evaluated for the treatment of PCa in a phase I clinical trial. In this clinical trial, patients with advanced-stage PCa received up to four cycles of GL-ONC1 administered intraperitoneally. Treatment was well tolerated and viral replication in the peritoneal cavity was detected only after the first administration.[40] A granulocyte-macrophage colony-stimulating factor-armed oncolytic vaccinia virus has been evaluated in the PCa MC38 model. The recombinant virus alone triggered antitumor immunity that could be enhanced by co-administration of monoclonal antibodies blocking programmed cell death protein 1 (PD-1) or lymphocyte-activation gene 3 (LAG-3).[41] In contrast to these previous reports, the MVA used in our study is a highly attenuated cytopathic strain. The lack of oncolytic capacity makes the virus less effective as monotherapy. In fact, the MVA.empty control virus fails to upregulate the antitumor immune response or mediate antitumor effects in our experimental setting. However, the capacity of MVA to accommodate large transgene inserts has been exploited to overexpress tumor-associated antigens alone or in combination with immunostimulatory molecules. Using these strategies, potent antitumor vaccines can be developed with a good safety profile.[23 24 26 42] However, the identification of tumor-associated neoantigens in PCa is challenging to timely formulate individual vaccines. Therefore, our objective was to design a tumor-agnostic strategy by overexpressing the highly T-cell-stimulating cytokine IL-12 cloned into the MVA vector. Interestingly, this MVA encoding scIL-12 was able to induce tumor-specific T lymphocytes in both the peritoneal cavity and the spleen, therefore suggesting the development of a systemic immune response. This adaptive immune response was able to completely eradicate MC38 cells implanted in the peritoneal cavity in a CD8-dependent manner. Furthermore, cured mice were protected against rechallenge with *s.c.* injection of MC38.

Intraperitoneal administration of MVA.scIL-12 was more effective than *i.v.* administration in terms of the elicited immune response and antitumor effect and mitigated the toxicity associated with scIL-12 when the vector was administered *i.v.* Furthermore, *i.p.* administration was able to control both peritoneal and subcutaneous tumors, while intratumor administration only controlled the progression of the treated subcutaneous lesions. This aspect could be advantageous for addressing peritoneal carcinomatosis originating from extraperitoneal primary tumors.[43] To explain the superiority of *i.p.* administration, we evaluated the targeting of MVA after *i.p.* and *i.v.* administration of an MVA encoding luciferase. After *i.v.* injection, the organs displaying the highest expression was the spleen, and bioluminescence in the mesentery and omentum was 10 times less intense. Peculiarly, *i.p.* administration leads to selectively high expression in the omentum with reduced expression in the spleen and mesentery. Therefore, MVA provides a useful tool to deliver IL-12 or perhaps other immunostimulatory transgenes selectively to the omentum. This is considered an advantage because the omentum is a key organ in the orchestration of the immune responses in the peritoneum.[44] Viral vectors targeting the omentum have not previously been reported with other vectors, but due to the role of this tissue in antiviral defense, it should be a general feature of gene therapy vectors infused into the peritoneal cavity. The relevance of the omentum in cancer immunotherapy must be taken into account when estimating the appropriateness of omentectomy in patients with PCa. This is especially true when considering the increasing number of clinical trials evaluating different forms of immunotherapy in this setting. In line with our research, a recent study by Christian *et al* has demonstrated that cDC1s resident in the omentum are able to coordinate innate responses to microbial challenges and provide secondary signals required for CD8 T-cell expansion and memory differentiation.[45] Indeed, surgical removal of omentum in our experimental setting reduced the antitumor effect (figure 4C). Our study reinforces the notion that the omentum is relevant in the induction of an effective locoregional and distant antitumor immune response when immunotherapy based on rMVA.scIL-12 is administered by *i.p.* injection.

In conclusion, our data support further evaluation in clinical trials in patients with PCa of *i.p.* administration of MVA vectors encoding scIL-12 due to the potent antitumor activity elicited by overexpression of IL-12 in the omentum. This local/regional strategy holds promise given the fact of its preclinical efficacy and because of the limited systemic exposure to IL-12-elicited IFN-γ that is a source of safety concerns.

Author affiliations
[1]Program of Immunology and Immunotherapy, Cima Universidad de Navarra, Pamplona, Spain
[2]Navarra Institute for Health Research (IDISNA), Pamplona, Spain
[3]Bavarian Nordic GmbH, Martinsried, Germany
[4]Centro de Investigación Biomédica en Red de Cáncer (CIBERONC), Madrid, Spain
[5]Department of Oncology and Department of Immunology and Immunotherapy, Clínica Universidad de Navarra, Pamplona, Spain
[6]Nuffield Department of Medicine and Oxford Center for Immuno-Oncology, University of Oxford, Oxford, UK

Twitter Alvaro Teijeira @itlive

Acknowledgements The authors thank Dr Paul Miller for English editing. We thank Dr Sandra Hervás-Stubbs for her advice regarding tetramer staining in the cytometry experiments. We also thank the Morphology and Cytometry Core Facility (CIMA-Universidad de Navarra) for technical support.

Contributors PB and FA designed the experiments and are guarantors. AB performed the experiments and processed samples. CA, JM-E, MH, and HH provided MVA.empty and MVA.scIL-12. PB performed all statistical analyses. AB, PB, and FA analyzed the data. AB, IM, PB, and FA wrote the manuscript. JG-G performed all bioinformatics analyses. All authors critically reviewed the manuscript for important intellectual content before final approval of the same.

Funding This study was supported by Bavarian Nordic, Instituto de Salud Carlos III (PI23/00203, PI22/00147 and PI20/00002) co-financed by Fondos Feder, Gobierno de Navarra Proyecto ARNMUNE Ref.: 0011–1411-2023, and Joint Translational Call for Proposals 2015 (JTC 2015) TRANSCAN-2 (code: TRS-2016-00000371). Work produced with the support of a 2022 Leonardo Grant for Researchers and Cultural Creators (BBVA Foundation). This project has received funding from the

European Union's Horizon 2020 research and innovation program under the Marie Skłodowska-Curie grant agreement No 765394. MA was supported by the Spanish Association against cancer research (AECC-2019 Investigator). FA receives a Miguel Servet I (CP19/00114) contract from ISCIII (Instituto de Salud Carlos III) co-financed by FSE (Fondo Social Europeo). AB is the recipient of PFIS fellowship from ISCIII (FI20/00058), and LA is the recipient of an FPU grant (FPU21/00042) from The Spanish Ministry of Education and Professional training. AT has received financial support through PID2020-113174-RA-100 (MCIN/ AEI /10.13039/501100011033) and RYC2019-026406-I/AEI/10.13039/501100011033 Fondo Social Europeo "El Fondo Social Europeo invierte en tu futuro"'.

Competing interests IM reports advisory roles with Roche-Genentech, Bristol-Myers Squibb, CYTOMX, Incyte, MedImmune, Tusk, F-Star, Genmab, Molecular Partners, Alligator, Bioncotech, MSD, Merck Serono, Boehringer Ingelheim, AstraZeneca, Numab, Catalym, and Bayer, and research funding from Roche, BMS, Alligator, and Highlight Therapeutics. PB and FA received research funding from Bavarian Nordic. CA, JM-E (former), MH, and HH are employees of Bavarian Nordic. The rest of the authors have no conflict of interest to declare.

Patient consent for publication Not applicable.

Ethics approval Experiments involving mice were approved by the Ethics Committee of the University of Navarra (033-20, 038-20, 063-21, and 014-21).

Provenance and peer review Not commissioned; externally peer reviewed.

Data availability statement Data are available upon reasonable request.

ORCID iDs
Maite Alvarez http://orcid.org/0000-0002-5969-9181
Alvaro Teijeira http://orcid.org/0000-0002-7339-4464
Maria Hinterberger http://orcid.org/0000-0003-2672-9134
Ignacio Melero http://orcid.org/0000-0002-1360-348X
Pedro Berraondo http://orcid.org/0000-0001-7410-1865
Fernando Aranda http://orcid.org/0000-0002-9364-474X

REFERENCES

1 Coccolini F, Gheza F, Lotti M, *et al*. Peritoneal carcinomatosis. *World J Gastroenterol* 2013;19:6979–94.
2 Cavaliere F, Giannarelli D, Valle M, *et al*. Peritoneal carcinomatosis from ovarian epithelial primary: combined aggressive treatment. *In Vivo* 2009;23:441–6.
3 van Baal JOAM, van Noorden CJF, Nieuwland R, *et al*. Development of peritoneal carcinomatosis in epithelial ovarian cancer: a review. *J Histochem Cytochem* 2018;66:67–83.
4 Kranenburg O, van der Speeten K, de Hingh I. Peritoneal metastases from colorectal cancer: defining and addressing the challenges. *Front Oncol* 2021;11:650098.
5 Terzi C, Arslan NC, Canda AE. Peritoneal carcinomatosis of gastrointestinal tumors: where are we now *World J Gastroenterol* 2014;20:14371–80.
6 Platell C, Cooper D, Papadimitriou JM, *et al*. The Omentum. *World J Gastroenterol* 2000;6:169–76.
7 Rangel-Moreno J, Moyron-Quiroz JE, Carragher DM, *et al*. Omental milky spots develop in the absence of lymphoid tissue-inducer cells and support B and T cell responses to peritoneal antigens. *Immunity* 2009;30:731–43.
8 Meza-Perez S, Randall TD. Immunological functions of the Omentum. *Trends Immunol* 2017;38:526–36.
9 Liu M, Silva-Sanchez A, Randall TD, *et al*. Specialized immune responses in the peritoneal cavity and Omentum. *J Leukoc Biol* 2021;109:717–29.
10 Mebius RE. Lymphoid organs for peritoneal cavity immune response: milky spots. *Immunity* 2009;30:670–2.
11 Krishnan V, Tallapragada S, Schaar B, *et al*. Omental macrophages secrete chemokine ligands that promote ovarian cancer colonization of the Omentum via CCR1. *Commun Biol* 2020;3:524.
12 Etzerodt A, Moulin M, Doktor TK, *et al*. Tissue-resident macrophages in Omentum promote metastatic spread of ovarian cancer. *J Exp Med* 2020;217:e20191869.
13 Lee W, Ko SY, Mohamed MS, *et al*. Neutrophils facilitate ovarian cancer premetastatic niche formation in the Omentum. *J Exp Med* 2019;216:176–94.
14 Francis P, Rowinsky E, Schneider J, *et al*. Phase I feasibility and pharmacologic study of weekly intraperitoneal paclitaxel: a gynecologic oncology group pilot study. *J Clin Oncol* 1995;13:2961–7.
15 Malfroy S, Wallet F, Maucort-Boulch D, *et al*. Complications after cytoreductive surgery with hyperthermic intraperitoneal chemotherapy for treatment of peritoneal carcinomatosis: risk factors for ICU admission and morbidity prognostic score. *Surg Oncol* 2016;25:6–15.
16 Burnett A, Lecompte M-EA, Trabulsi N, *et al*. Peritoneal carcinomatosis index predicts survival in colorectal patients undergoing HIPEC using Oxaliplatin: a retrospective single-arm cohort study. *World J Surg Oncol* 2019;17:83.
17 Zhang C, Wang Z, Yang Z, *et al*. Phase I escalating-dose trial of CAR-T therapy targeting CEA^+ metastatic colorectal cancers. *Mol Ther* 2017;25:1248–58.
18 Koneru M, O'Cearbhaill R, Pendharkar S, *et al*. A phase I clinical trial of adoptive T cell therapy using IL-12 secreting MUC-16(Ecto) directed Chimeric antigen receptors for recurrent ovarian cancer. *J Transl Med* 2015;13:102.
19 Morano WF, Aggarwal A, Love P, *et al*. Intraperitoneal immunotherapy: historical perspectives and modern therapy. *Cancer Gene Ther* 2016;23:373–81.
20 Heery C, Pico-Navarro C, Adams T, *et al*. 4P - Novel applications of MVA to improve outcomes in Immunooncology. *Ann Oncol* 2019;30:i3.
21 Frank MJ, Reagan PM, Bartlett NL, *et al*. In situ vaccination with a TLR9 agonist and local low-dose radiation induces systemic responses in untreated indolent lymphoma. *Cancer Discov* 2018;8:1258–69.
22 Dai P, Wang W, Cao H, *et al*. Modified vaccinia virus Ankara triggers type I IFN production in murine conventional dendritic cells via a cGAS/STING-mediated cytosolic DNA-sensing pathway. *PLoS Pathog* 2014;10:e1003989.
23 Hinterberger M, Giessel R, Fiore G, *et al*. Intratumoral virotherapy with 4-1BBL armed modified vaccinia ankara eradicates solid tumors and promotes protective immune memory. *J Immunother Cancer* 2021;9:e001586.
24 Medina-Echeverz J, Hinterberger M, Testori M, *et al*. Synergistic cancer immunotherapy combines MVA-CD40L induced innate and adaptive immunity with tumor targeting antibodies. *Nat Commun* 2019;10:5041.
25 Tenesaca S, Vasquez M, Alvarez M, *et al*. Statins act as transient type I interferon inhibitors to enable the antitumor activity of modified vaccinia ankara viral vectors. *J Immunother Cancer* 2021;9:e001587.
26 Pittman PR, Hahn M, Lee HS, *et al*. Phase 3 efficacy trial of modified vaccinia ankara as a vaccine against smallpox. *N Engl J Med* 2019;381:1897–908.
27 Berraondo P, Etxeberria I, Ponz-Sarvise M, *et al*. Revisiting interleukin-12 as a cancer immunotherapy agent. *Clin Cancer Res* 2018;24:2716–8.
28 Jung K, Ha J-H, Kim J-E, *et al*. Heterodimeric FC-fused Il12 shows potent antitumor activity by generating memory CD8(+) T cells. *Oncoimmunology* 2018;7:e1438800.
29 Skrombolas D, Sullivan M, Frelinger JG. Development of an Interleukin-12 fusion protein that is activated by cleavage with matrix metalloproteinase 9. *J Interferon Cytokine Res* 2019;39:233–45.
30 Xue D, Moon B, Liao J, *et al*. A tumor-specific pro-IL-12 activates preexisting cytotoxic T cells to control established tumors. *Sci Immunol* 2022;7:eabi6899.
31 Etxeberria I, Bolaños E, Quetglas JI, *et al*. Intratumor adoptive transfer of IL-12 mRNA transiently engineered antitumor $CD8^+$ T cells. *Cancer Cell* 2019;36:613–29.
32 Hewitt SL, Bailey D, Zielinski J, *et al*. Intratumoral IL12 mRNA therapy promotes TH1 transformation of the tumor microenvironment. *Clin Cancer Res* 2020;26:6284–98.

33 Agliardi G, Liuzzi AR, Hotblack A, *et al*. Intratumoral IL-12 delivery empowers CAR-T cell immunotherapy in a pre-clinical model of glioblastoma. *Nat Commun* 2021;12:444.
34 Melero I, Castanon E, Alvarez M, *et al*. Intratumoural administration and tumour tissue targeting of cancer immunotherapies. *Nat Rev Clin Oncol* 2021;18:558–76.
35 Cirella A, Luri-Rey C, Di Trani CA, *et al*. Novel strategies exploiting Interleukin-12 in cancer immunotherapy. *Pharmacol Ther* 2022;239:108189.
36 Liao Y, Smyth GK, Shi W. featureCounts: an efficient general purpose program for assigning sequence reads to genomic features. *Bioinformatics* 2014;30:923–30.
37 Langmead B, Salzberg SL. Fast Gapped-read alignment with Bowtie 2. *Nat Methods* 2012;9:357–9.
38 Robinson MD, McCarthy DJ, Smyth GK. edgeR: a Bioconductor package for differential expression analysis of digital gene expression data. *Bioinformatics* 2010;26:139–40.
39 Korotkevich G, Sukhov V, Budin N, *et al*. Fast gene set enrichment analysis. *Bioinformatics* [Preprint].
40 Lauer UM, Schell M, Beil J, *et al*. Phase I study of oncolytic vaccinia virus GL-ONC1 in patients with peritoneal carcinomatosis. *Clin Cancer Res* 2018;24:4388–98.
41 Lee YS, Lee WS, Kim CW, *et al*. Oncolytic vaccinia virus reinvigorates peritoneal immunity and cooperates with immune checkpoint inhibitor to suppress peritoneal carcinomatosis in colon cancer. *J Immunother Cancer* 2020;8:e000857.
42 Guo ZS, Lu B, Guo Z, *et al*. Vaccinia virus-mediated cancer immunotherapy: cancer vaccines and oncolytics. *J Immunother Cancer* 2019;7:6.
43 Rijken A, Galanos LJK, Burger JWA, *et al*. Peritoneal metastases from extraperitoneal primary tumors: incidence, treatment, and survival from a nationwide database. *Indian J Surg Oncol* 2023;14:60–6.
44 Liu Y, Hu J, Luo N, *et al*. The essential involvement of the Omentum in the peritoneal defensive mechanisms during intra-abdominal sepsis. *Front Immunol* 2021;12:631609.
45 Christian DA, Adams TA II, Shallberg LA, *et al*. CDC1 coordinate innate and adaptive responses in the Omentum required for T cell priming and memory. *Sci Immunol* 2022;7:75.